American Heart Journal Plus: Cardiology Research and Practice 35 (2023) 100328

Contents lists available at ScienceDirect

American Heart Journal Plus: Cardiology Research and Practice

journal homepage: www.sciencedirect.com/journal/american-heart-journal-plus-cardiology-research-and-practice

Research Paper

Energy loss is related to CT fractional flow reserve progression in type 2 diabetes mellitus patients☆

Nobuo Tomizawa [a,*], Shinichiro Fujimoto [b], Daigo Takahashi [b], Yui Nozaki [b], Ruiheng Fan [a], Ayako Kudo [b], Yuko Kawaguchi [b], Kazuhisa Takamura [b], Makoto Hiki [b], Satoshi Kadowaki [c], Fuki Ikeda [c], Kanako K. Kumamaru [a], Hirotaka Watada [c], Tohru Minamino [b], Shigeki Aoki [a]

[a] Department of Radiology, Juntendo University Graduate School of Medicine, Tokyo, Japan
[b] Department of Cardiovascular Biology and Medicine, Juntendo University Graduate School of Medicine, Tokyo, Japan
[c] Department of Diabetes, Endocrinology, and Metabolism, Juntendo University Graduate School of Medicine, Tokyo, Japan

ARTICLE INFO

Keywords:
CT angiography
Computational modeling
Coronary artery stenosis
Energy loss
Fractional flow reserve

ABSTRACT

Background: We aimed to investigate the diagnostic value of energy loss (EL) and baseline CT fractional flow reserve (CT-FFR) computed using computational fluid dynamics to predict functional progression of coronary stenosis in patients with type 2 diabetes mellitus.

Methods: This single-center prospective study included 61 patients with type 2 diabetes mellitus (mean age, 61 years ±9 [SD]; 43 men) showing 20–70 % stenosis who underwent serial coronary CT performed at 2-year interval between October 2015 and March 2020. A mesh-free simulation was performed to calculate the CT-FFR and EL. Functional progression was defined as ≥ 0.05 decrease in CT-FFR on the second coronary CT. Models using baseline CT-FFR and EL were compared by analyzing the receiver operating characteristic (ROC) curve.

Results: Of the 94 vessels evaluated, 25 vessels (27 %) showed functional progression. EL at distal stenosis (EL_{dis}) of vessels with functional progression was higher than that of vessels without functional progression (27.6 W/m^3 [interquartile range (IQR): 15.0, 53.0] vs. 5.7 W/m^3 [IQR: 2.3, 10.1], $p < 0.001$). Multivariable analysis showed that EL_{dis} (per unit Ln(EL); odds ratio, 11.8; 95 % CI: 4.0–34.9; $p < 0.001$) remained as a predictor of functional progression after adjustment for diameter stenosis and baseline CT-FFR. The area under the ROC curve using EL_{dis} (0.89; 95 % CI: 0.82–0.96) was higher than that using baseline CT-FFR (0.71; 95 % CI: 0.59–0.83; $p < 0.001$).

Conclusion: When EL_{dis} and baseline CT-FFR were considered, EL_{dis} was a better predictor of functional progression of coronary stenosis.

1. Introduction

The improvement of computational capabilities has allowed the introduction of computational fluid dynamics (CFD) in the field of cardiovascular medicine [1]. Of note, fractional flow reserve (FFR) derived from CT data has become a new standard to non-invasively diagnose functionally significant stenosis [2]. A recent meta-analysis showed that the per-vessel sensitivity and specificity of CT-FFR to diagnose functionally significant stenosis was 85 % and 82 %, respectively [3]. Although several studies showed the prognostic value of CT-FFR [4–6], lesion-specific evaluation is difficult because CT-FFR value is calculated on a per-vessel basis. In addition, lesion-specific evaluation using ΔCT-FFR has been shown to predict early revascularization but has not been investigated to predict longitudinal plaque progression [7].

In addition to pressure calculation, coronary blood flow velocity could also be derived from CFD analysis. Velocity data can be used to calculate CFD indices such as wall shear stress, vorticity, kinetic energy, and viscous energy loss (EL) [8]. Viscous EL has received attention in 4D flow MRI studies. These studies showed that viscous EL was related to abnormal flow in patients with aortic aneurysm [9], aortic valvular

Abbreviations: AUC, area under the curve; CFD, computational fluid dynamics; DS, diameter stenosis; EL, energy loss; FFR, fractional flow reserve; IQR, interquartile range; OR, odds ratio; ROC, receiver operating characteristic.

☆ This study was performed in Tokyo, Japan.

* Corresponding author at: Department of Radiology, Juntendo University Graduate School of Medicine, 2-1-1, Hongo, Bunkyo-ku, 113-8421 Tokyo, Japan.
E-mail address: tomizawa-tky@umin.ac.jp (N. Tomizawa).

https://doi.org/10.1016/j.ahjo.2023.100328
Received 24 September 2023; Accepted 25 September 2023
Available online 28 September 2023

disease [10,11], and repaired tetralogy of Fallot [12]. Viscous EL might have a potential to predict future plaque progression in coronary artery disease, but measuring EL is a challenge using MRI due to spatial resolution issues. Furthermore, factors that contribute to the progression of coronary artery disease in terms of a decrease in FFR has not been fully investigated. Investigating factors for functional progression is important to predict the likelihood of future revascularization procedures. We assumed that EL calculated using coronary CT data could better predict the functional progression of coronary plaque than CT-FFR. Additionally, diabetes mellitus is a risk factor for distribution and progression of coronary artery disease [13]. The prevalence of obstructive coronary artery disease and high-risk plaques is higher in patients with diabetes mellitus than in those with hypertension or dyslipidemia [14]. Plaques are more likely to progress with greater severity of diabetes mellitus [15]. Therefore, the purpose of the present study was to compare the value of EL and CT-FFR to predict functional progression of coronary plaque using data from serial coronary CT performed at 2-year intervals in patients with type 2 diabetes mellitus.

2. Methods

2.1. Patients

This single-center prospective study was approved by the institutional review board and written informed consent was provided by all patients. We initially included 452 consecutive patients with type 2 diabetes mellitus between the ages of 35 and 70 years old who were offered a one-week in-hospital diabetes education program between October 2015 and March 2020 (Fig. 1). The exclusion criteria were as follows: known coronary artery disease ($n = 97$), asthma ($n = 15$), severe aortic valve stenosis ($n = 4$), allergy to contrast medium ($n = 5$), poor kidney function ($n = 62$). A total of 70 patients did not give consent to perform the first coronary CT scan and another 89 patients withdrew from the study before the second coronary CT scan. Therefore, serial coronary CT was performed at 2-year interval in 110 patients. In addition, 48 patients without plaques with ≥20 % stenosis and one patient who had undergone coronary artery bypass grafting were excluded. Therefore, the final study group included 61 patients. Of the eligible 183 vessels, 94 vessels with 20–70 % stenosis in the initial CT were analyzed. If multiple plaques were present, the most proximal plaque was considered.

We defined diabetes mellitus, hypertension, and dyslipidemia as follows: (1) diabetes mellitus, fasting glucose level ≥ 126 mg/dl and/or hemoglobin A1c ≥ 6.5 % and/or need for insulin or oral antidiabetic drugs) [16]; (2) hypertension, blood pressure ≥ 140/90 mmHg and/or use of antihypertensive drugs; (3) dyslipidemia (low-density lipoprotein ≥ 140 mg/dl and/or high-density lipoprotein ≤ 40 mg/dl and/or triglyceride ≥ 150 mg/dl and/or need for antilipidemic drugs) [17].

2.2. Coronary CT angiography

A 320-row CT was used to perform coronary CT angiography (Aquilion ONE Genesis Edition; Canon Medical Systems Corporation). Oral β-blocker (metoprolol, 20 or 40 mg) was used 1 h before the exam to achieve the target heart rate of 65 beats per minute. A maximum dose of 12.5 mg of landiolol (Corebeta; Ono Parmaceutical) was given intravenously if the heart rate was > 65 bpm at the CT room [18]. All patients received 0.6 mg of sublingual nitroglycerin (Nitropen; Nippon Kayaku) before imaging. Patients received 18.0 mg iodine/kg/s of iomeprol (Iomeron 350; Eisai) for 12 s, followed by a 30 ml saline flush. Images were reconstructed with slice thickness and increment of 0.50 mm and 0.25 mm, respectively, using a convolution kernel of FC04 with iterative reconstruction (AIDR 3D [adaptive iterative dose reduction using a three-dimensional processing algorithm]; Canon Medical Systems Corporation). Images were transferred to a workstation for post-processing (Synapse Vincent, version 6.0; Fujifilm Medical).

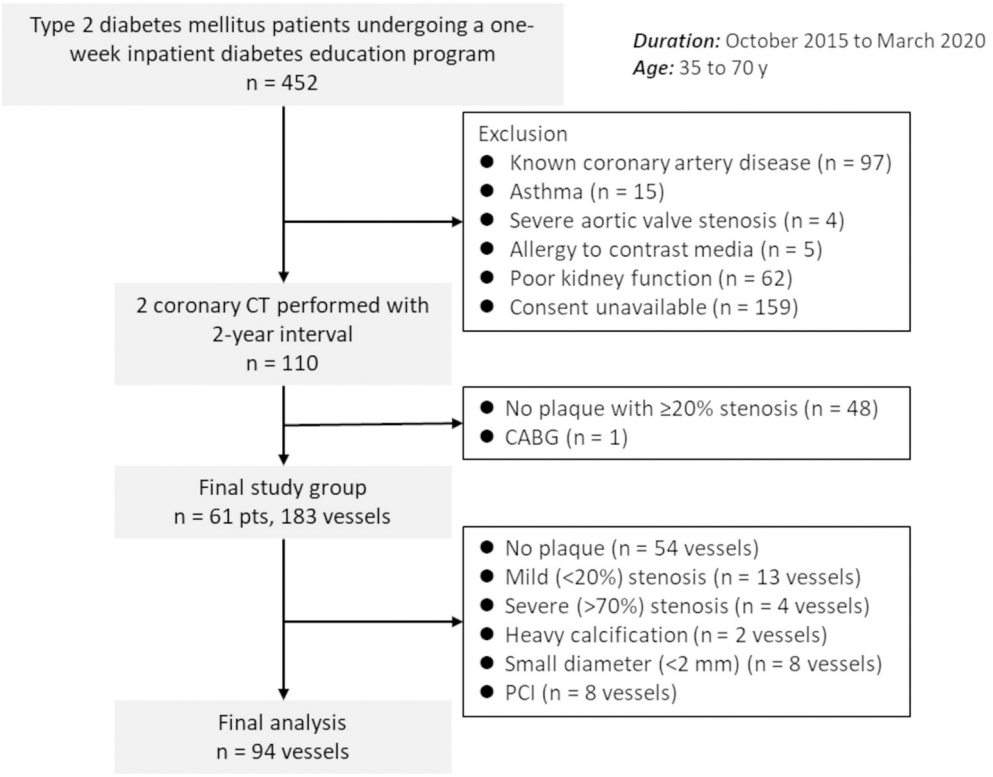

Fig. 1. Patient flowchart. The study initially included 452 consecutive patients undergoing a one-week inpatient diabetes education program. Consecutive coronary CTs with 2-year interval were performed on 110 patients. The final analysis included 61 patients and 94 vessels with 20–70 % stenosis.
CABG = coronary artery bypass grafting; PCI = percutaneous coronary intervention; pts. = patients.

2.3. Coronary stenosis analysis

Stenosis analysis software in the workstation automatically identified the lumen border. Diameter stenosis (DS) was automatically obtained. Left ventricular myocardial volume of the stenosis related territory was estimated by performing myocardial segmentation using the Voronoi method (Myocardial analysis; Fujifilm Medical) [19].

2.4. CFD analysis

We used a mesh-free method (OpenMPS) to perform CFD analysis. The OpenMPS software is an open-source implementation of moving particle semi-implicit method available at GitHub (https://github.com/OpenMps/openmps) [20]. In brief, a three-dimensional CFD algorithm was employed from approximately 1 cm proximal to 2 cm distal to the stenosis. The CT-FFR value at 2 cm distal to the stenosis was recorded (Fig. 2). If the CT-FFR decreased by ≥ 0.05 on the second CT, the stenosis was considered to be functionally progressive. This cutoff value was set first to exclude interobserver error [21] and second because a 0.05 decrease in CT-FFR would increase the liklihood of future revascularization [7]. Energy loss (EL, in W/m^3) of the following 4 points were acquired: proximal, middle, and distal thirds of the lesion; entire lesion (Fig. 2). EL was calculated as follows [22]:

$$EL = \frac{1}{V}\int_V \mu\phi dV \tag{1}$$

where μ is fluid viscosity (4.2×10^{-3} Pa s) and ϕ can be derived as follows:

$$\phi = 2\sum_{i=1}^{3}\left(\frac{\partial u_i}{\partial x_i}\right)^2 + \sum_{i,j=1,i\neq j}^{3}\left(\frac{\partial u_i}{\partial x_j}+\frac{\partial u_j}{\partial x_i}\right)^2 - \frac{2}{3}\left(\sum_{i=1}^{3}\frac{\partial u_i}{\partial x_i}\right)^2 \tag{2}$$

Measurements were performed by a cardiovascular radiologist (N.T., with 15 years of experience). As a second observer, a radiation technician (R.F., with 5 years of experience) measured these values in the randomly selected 30 vessels.

2.5. Statistical analysis

Continuous variables were shown as means ± SDs and categorical variables as numbers with percentages, unless otherwise described. Student *t*-test was used to compare continuous variables. The Fisher exact test and Wilcoxon test were used to compare categorical variables and skewed variables, respectively. The McNemar test was used to compare the accuracy of each potential risk factor in detecting functional progression. We adjusted the multiple vessels per patient. Intraclass correlation coefficient was used to investigate inter-observer variability for EL.

Pearson's correlation analysis was used to investigate the relationship between CT-FFR decrease in 2 years and EL. Logistic regression analysis was used to predict functional progression. EL values were converted to Ln(EL) for normalization. Variables with $p < 0.10$ in univariable analysis were included in multivariable analysis. As for EL, the segment with the highest odds ratio (OR) was included in multivariable analysis. Generalized estimated equations were used to adjust multiple vessels per patient. Receiver operating characteristic (ROC) curve analysis was used to compare the predictive value of CT-FFR and EL. The Youden index was used to determine the optimal cutoff value.

A total of 94 vessels were included in this study, which provided 78 % power ($\alpha = 0.05$) to detect superiority in the area under the curve (AUC) of CT-FFR vs. EL of distal stenosis.

Differences in AUC values were assessed using the DeLong method using the logistic regression analysis adjusted for multiple vessels per patient. Logistic regression analysis, DeLong method, and calculation of ICCs were performed using R software (version 4.0.2; R Foundation for Statistical Computing). The remaining statistical analyses were performed using JMP software, version 17.0.0 (SAS institute). A *p*-value < 0.05 was considered to indicate a statistically significant difference.

3. Results

3.1. Patient and lesion characteristics

Our study included 61 patients (mean age, 61 years ±9 [SD]; 43 men) (Table 1). All patients had diabetes mellitus. Hypertension and dyslipidemia were present in 24 patients (39 %) and 39 patients (64 %), respectively. More than half of the patients (43 patients, 70 %) had a smoking history. Statin was prescribed in 40 patients (66 %).

In order of decreasing frequency, coronary stenoses were located in the left anterior descending artery (50 vessels, 53 %), right coronary artery (27 vessels, 29 %), and left circumflex artery (17 vessels, 18 %) (Table 2). The mean DS was 31.6 % ± 9.6.

3.2. Baseline CT-FFR and EL

The mean baseline CT-FFR was 0.85 ± 0.15, and 25 of 94 vessels (27

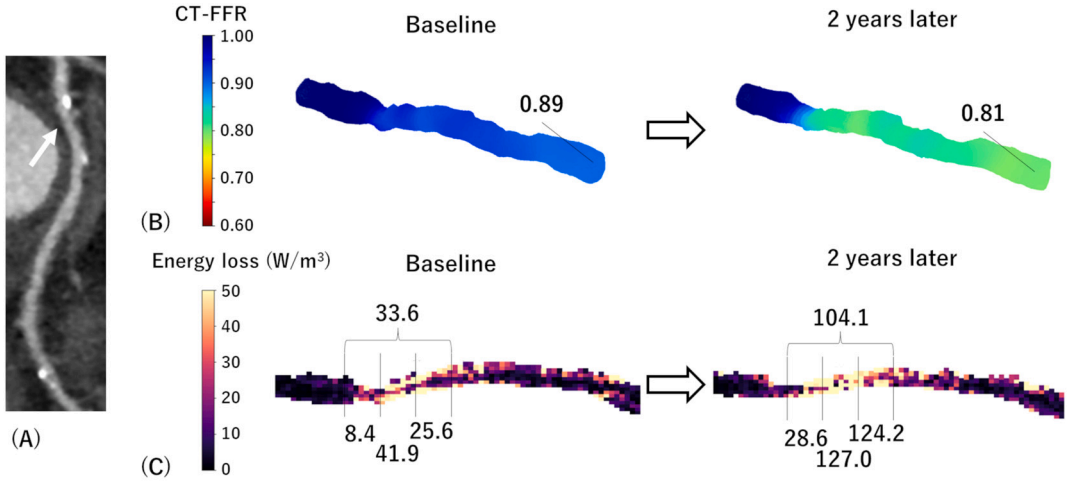

Fig. 2. Images in a 69-year-old male with functional progression in 2 years. Mild stenosis with calcified plaque was present in the proximal left circumflex artery (A). The baseline CT-FFR was 0.89, which progressed to 0.81 in 2 years (B). The energy loss of the distal segment of stenosis progressed from 25.6 W/m^3 to 124.2 W/m^3 (C).
CT-FFR = CT fractional flow reserve.

Table 1
Patient demographics.

No. of patients	61
Male	43 (71 %)
Age (y)	60.6 ± 8.6
Body mass index (kg/m^2)	26.6 ± 4.7
Cardiac risk factors	
Hypertension	24 (39 %)
Diabetes mellitus	61 (100 %)
Dyslipidemia	39 (64 %)
Smoking, current/ex	21/22 (34 %/36 %)
Family history	16 (27 %)
Medication	
Statin	40 (66 %)
Oral hypoglycemic agents	49 (80 %)
Insulin	20 (33 %)

Numbers are reported as mean ± SD or number of patients with percentages in parentheses.

Table 2
Lesion characteristics.

Parameter	All vessels	Functional no progression (ΔCT-FFR < 0.05)	Functional progression (ΔCT-FFR ≥ 0.05)	p
Vessel	94	69	25	
Left anterior descending	50 (53 %)	18 (72 %)	32 (46 %)	0.08
Left circumflex	17 (18 %)	2 (8 %)	15 (22 %)	
Right coronary	27 (29 %)	5 (20 %)	22 (32 %)	
DS (%)	31.6 ± 9.6	30.6 ± 10.0	34.6 ± 7.8	0.07
Baseline CT-FFR	0.85 ± 0.15	0.87 ± 0.15	0.80 ± 0.14	0.04*
Energy loss (W/m^3)[a]				
Proximal stenosis	5.3 (2.4, 11.4)	3.7 (1.8, 9.6)	11.5 (8.5, 19.9)	<0.001*
Middle stenosis	11.2 (4.4, 31.4)	7.2 (3.5, 16.3)	38.9 (13.6, 51.5)	<0.001*
Distal stenosis	8.5 (3.1, 20.0)	5.7 (2.3, 10.1)	27.6 (15.0, 53.0)	<0.001*
Entire stenosis	9.7 (3.2, 23.0)	6.1 (2.6, 12.6)	31.0 (11.9, 39.3)	<0.001*

Numbers are reported as mean ± SD or number of patients with percentages in parentheses, unless otherwise noted.
DS = diameter stenosis, FFR = fractional flow reserve.
* Statistically significant, $p < 0.05$.
[a] Numbers are reported as median with interquartile range in parentheses.

%) showed functional progression (ΔCT-FFR ≥0.05) (Table 2). Vessels with functional progression had lower baseline CT-FFR values than the remaining vessels (0.80 ± 0.14 vs. 0.87 ± 0.15, $p = 0.04$). The median EL in vessels with functional progression was higher than that without functional progression in proximal (11.5 W/m^3 [interquartile range (IQR): 8.5, 19.9] vs. 3.7 W/m^3 [IQR: 1.8, 9.6], $p < 0.001$), middle (38.9 W/m^3 [IQR: 13.6, 51.5] vs. 7.2 W/m^3 [IQR: 3.5, 16.3], $p < 0.001$), distal (27.6 W/m^3 [IQR: 15.0, 53.0] vs. 5.7 W/m^3 [IQR: 2.3, 10.1], $p < 0.001$), and entire stenosis (31.0 W/m^3 [IQR: 11.9, 39.3] vs. 6.1 W/m^3 [IQR: 2.6, 12.6], $p < 0.001$). Pearson's correlation analysis showed a positive relationship between EL_{dis} and CT-FFR decrease in 2 years (Fig. 3).

Increase in EL after 2 years was larger in vessels with functional progression than in the remaining vessels in proximal (3.5 W/m^3 [IQR: 8.8, 62.6] vs. −0.2 W/m^3 [IQR: −4.0, 2.9], $p < 0.001$), middle (24.9 W/m^3 [IQR: 8.8, 62.6] vs. −0.2 W/m^3 [IQR: −2.7, 3.2], $p < 0.001$), distal (5.7 W/m^3 [IQR: −1.6, 39.8] vs. 0.0 W/m^3 [IQR: −2.7, 3.2], $p < 0.001$), and entire stenosis (18.6 W/m^3 [IQR: 5.7, 36.8] vs. −0.3 W/m^3 [IQR: −3.2, 2.2], $p < 0.001$) (Supplemental Table 1).

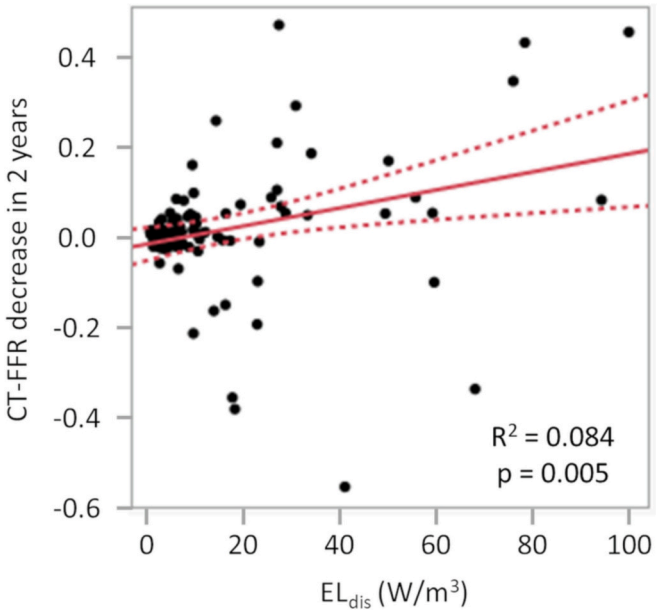

Fig. 3. Scatter plot showing the relationship between EL_{dis} and CT-FFR decrease in 2 years. Although the relationship was weak ($R^2 = 0.084$), the relationship was significant ($p = 0.005$).
CT-FFR = CT fractional flow reserve; EL_{dis} = energy loss at distal stenosis.

Interobserver intraclass correlation coefficients of CT-FFR and EL of proximal, middle, distal, and entire stenosis were 0.96 (95 % CI: 0.91–0.98), 0.88 (95 % CI: 0.77–0.94), 0.97 (95 % CI: 0.94–0.99), 0.96 (95 % CI: 0.92–0.98), and 0.96 (95 % CI: 0.93–0.98), respectively, indicating good agreement.

3.3. Logistic regression analysis

Univariable logistic regression analysis showed that EL of proximal (per unit ln(EL); OR, 4.75; 95 % CI: 2.43–9.27; $p < 0.001$), middle (OR, 2.57; 95 % CI: 1.55–4.28; p < 0.001), distal (OR, 6.05; 95 % CI: 3.06–12.0; p < 0.001), and entire stenosis (OR, 3.60; 95 % CI: 2.01–6.45; p < 0.001) were predictors of functional progression, while DS and baseline CT-FFR were not significant predictors (Table 3). When DS, baseline CT-FFR, and EL at distal stenosis were included in the multivariable analysis, baseline CT-FFR (per 0.05 decrease; OR, 0.78; 95 % CI: 0.60–0.99; $p = 0.04$) and EL at distal stenosis (OR, 11.8; 95 %

Table 3
Logistic regression analysis to predict functional progression (ΔCT-FFR ≥0.05).

Parameter	Univariable		Multivariable	
	Odds ratio (95 % CI)	p	Odds ratio (95 % CI)	p
DS (per 5 %)	1.24 (0.98–1.57)	0.08	0.93 (0.62–1.38)	0.72
Baseline CT-FFR (per 0.05 decrease)	1.16 (0.99–1.35)	0.06	0.78 (0.60–0.99)	0.04*
EL (per unit ln(EL))				
Proximal	4.75 (2.43–9.27)	<0.001*		
Middle	2.57 (1.55–4.28)	<0.001*		
Distal	6.05 (3.06–12.0)	<0.001*	11.8 (4.0–34.9)	<0.001*
Entire	3.60 (2.01–6.45)	<0.001*		

DS = diameter stenosis, EL = energy loss, FFR = fractional flow reserve.
* Statistically significant, p < 0.05.

CI: 4.0–34.9; $p < 0.001$) were predictors of functional progression.

3.4. ROC curve analysis and diagnostic performance

In the ROC curve predicting functional progression, the AUC of EL at distal stenosis (0.89; 95 % CI: 0.82–0.96) was higher than those of DS (0.66; 95 % CI: 0.55–0.77) and baseline CT-FFR (0.71; 95 % CI: 0.59–0.83; $p < 0.001$) (Fig. 4). The best cutoff values for DS, baseline CT-FFR, and EL at distal stenosis were 27 %, 0.87, and 19.0 W/m^3, respectively.

We found no evidence of difference in sensitivity to predict functional progression between models including DS, baseline CT-FFR, and EL at distal stenosis (Table 4). The specificity of DS and baseline CT-FFR were 48 % (33 out of 69 vessels; 95 % CI: 36–60) and 77 % (53 out of 69 vessels; 95 % CI: 65–86), respectively, which improved to 91 % (63 out of 69 vessels; 95 % CI: 82–97; $p < 0.001$) with EL at distal stenosis. The diagnostic accuracy of EL at distal stenosis (86 %; 81 of 94 vessels; 95 % CI: 78–92) was higher than those of DS (59 %; 55 out of 94 vessels; 95 % CI: 48–69; $p < 0.001$) and baseline CT-FFR (74 %; 70 of 94 vessels; 95 % CI: 64–83; $p = 0.007$).

4. Discussion

Patients who are admitted for diabetes education program often have poor glycemic control and are at risk for rapid progression of coronary artery disease [23]. Our study showed that EL was higher in vessels with functional progression than in the remaining vessels. The AUC of the ROC curve to predict functional progression in a model including EL at distal stenosis was higher than that of DS and baseline CT-FFR. The predictive value of EL at distal stenosis was higher than that of DS and baseline CT-FFR mainly by increasing the specificity. A previous study showed that coronary flow vorticity could predict progression of coronary plaques [21]. Since EL assessed in this study is an index to directly assess the transfer of fluid energy into the plaque, EL would be an ideal marker to investigate the progression of coronary plaques.

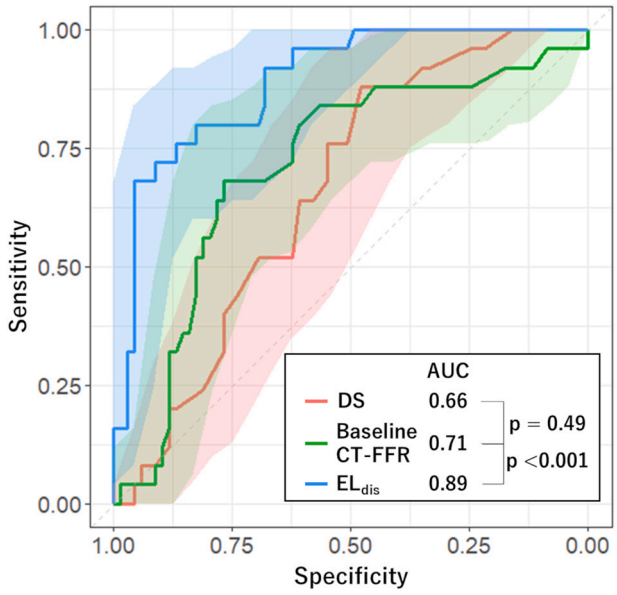

Fig. 4. Comparison of receiver operating characteristic curves to predict functional plaque progression. The areas under the receiver operating characteristic curve of models including DS and baseline CT-FFR were 0.66 (95 % CI: 0.55–0.77) and 0.71 (95 % CI: 0.59–0.83), respectively, which increased to 0.89 (95 % CI: 0.82–0.96; $p < 0.001$) with EL_{dis}. Shaded areas represent 95 % confidence band.
AUC = area under the curve; CT-FFR = CT fractional flow reserve; DS = diameter stenosis; EL_{dis} = energy loss at distal stenosis.

Table 4
Diagnostic performance to predict functional progression (ΔCT-FFR ≥0.05).

	DS	Baseline CT-FFR	EL_{dis}
Sensitivity	88 (22/25) [69–97]	68 (17/25) [46–85]	72 (18/25) [51–88]
Specificity	48 (33/69) [36–60]	77 (53/69) [65–86]	91 (63/69) [82–97]*,†
Positive predictive value	38 (22/58) [26–52]	52 (17/33) [34–69]	75 (18/24) [53–90]*
Negative predictive value	92 (33/36) [78–98]	87 (53/61) [76–94]	90 (63/70) [80–96]
Accuracy	59 (55/94) [48–69]	74 (70/94) [64–83]*	86 (81/94) [78–92]*,†

Data in parentheses are numbers of patients, with 95 % CIs in brackets.
DS = diameter stenosis, EL_{dis} = energy loss at distal stenosis, FFR = fractional flow reserve.
* Statistically significant (vs. DS), $p < 0.05$.
† Statistically significant (vs. baseline CT-FFR), $p < 0.05$.

It is well known that the prognosis of patients with obstructive coronary artery disease is worse than patients without [24]. However, there is a lack of evidence of morphological parameters such as DS to predict lesion specific progression. This is in line with the present study that the positive predictive value of DS was low. Therefore, CFD parameters have been studied to predict plaque progression. Longitudinal studies of CT-FFR have shown that lower CT-FFR values are associated with increased cardiovascular events [4,5,25]. However, these studies have not investigated lesion-specific outcomes, and Lee et al. conducted a case-control study to investigate whether hemodynamic characteristics could be responsible for subsequent acute coronary syndromes [26]. They showed that factors such as CT-FFR, wall shear stress, and axial plaque stress were shown to be predictors of future plaque rupture, but the AUC of the ROC curve in a model including these parameters was moderate (c-index 0.79). The sensitivity and specificity were approximately 70–80 %, similar to the values in our study in a model using CT-FFR. Therefore, the inclusion of EL would further strengthen the clinical impact of hemodynamic parameters to predict lesion-specific progression.

The presence of coronary stenosis causes disturbed flow, resulting in increased vorticity [27]. In this state, kinetic energy is partially converted to acoustic and thermal energy due to friction, viscosity, and turbulence [8,9]. High EL is related to increased wall shear stress [28], which induces platelet dysfunction that exacerbates the local thrombotic propensity [29]. High wall shear stress is associated with proinflammatory pathway which results in plaque progression [30]. From these findings, EL could be an ideal predictor for plaque progression.

Four-dimensional flow MRI is commonly used to directly examine blood flow [8,31]. The strength of MRI is that the blood flow is the actual value, and no ionizing radiation is necessary for acquisition [31]. However, the spatial resolution of MRI is inferior to CT and MRI might be difficult to reproduce small structures such as coronary plaques. Also, MRI acquisitions are performed for multiple heartbeats and the results are influenced by heartbeat variations. Although the acquisition of CT is quick, simulation of the cardiac flow might be time consuming. Conversely, the MRI results are available at the end of the scan. Therefore, the appropriate modality for analysis depends on the anatomy to analyze. When the structure is small and complex, CT might be superior to MRI for CFD analysis.

Our study had limitations. First, this was a single-center study using a single CT system. Multi-center study using various CT vendors is necessary to confirm the results of this study. Second, the results might change when other CFD methods are used. The CFD system we used is based on the Navier-Stokes equation, and the FFR values derived from this method has been verified against invasive FFR [20]. Third, only patients with type 2 diabetes mellitus was included in this study because diabetes mellitus is a stronger factor for plaque distribution and progression than other cardiovascular risk factors such as hypertension and

dyslipidemia [14,15]. Further study is necessary to investigate whether EL is a factor to predict functional progression in different patient characteristics. Fourth, this study did not aim to investigate factors to improve the prognosis of patients. Studies to focusing on therapeutic methods using CFD data would enhance the results of this study. Finally, the high drop-out rate of this study due to the coronary virus disease 2019 pandemic might have resulted in selection bias.

In conclusion, EL at distal stenosis was a better predictor than baseline CT-FFR in predicting functional progression of coronary stenosis. Assessing EL of coronary stenosis using coronary CT data calculated by CFD could non-invasively predict functional progression in patients with type 2 diabetes mellitus.

Supplementary data to this article can be found online at https://doi.org/10.1016/j.ahjo.2023.100328.

Acknowledgements

This work was supported by JSPS KAKENHI [Grant Number 21K07573].

References

[1] M.S. Nazir, T.K. Mittal, J. Weir-McCall, K. Nieman, K. Channon, E.D. Nicol, Opportunities and challenges of implementing computed tomography fractional flow reserve into clinical practice, Heart 106 (18) (2020 Sep) 1387–1393.
[2] B.L. Nørgaard, T.A. Fairbairn, R.D. Safian, M.G. Rabbat, B. Ko, J.M. Jensen, et al., Coronary CT Angiography-derived Fractional Flow Reserve Testing in Patients with Stable Coronary Artery Disease: Recommendations on Interpretation and Reporting. Radiol Cardiothorac Imaging [Internet] 1(5), 2019 Dec 1, e190050. Available from: https://doi.org/10.1148/ryct.2019190050.
[3] B. Zhuang, S. Wang, S. Zhao, M. Lu, Computed tomography angiography-derived fractional flow reserve (CT-FFR) for the detection of myocardial ischemia with invasive fractional flow reserve as reference: systematic review and meta-analysis, Eur. Radiol. 30 (2) (2020 Feb 6) 712–725.
[4] M.R. Patel, B.L. Nørgaard, T.A. Fairbairn, K. Nieman, T. Akasaka, D.S. Berman, et al., 1-year impact on medical practice and clinical outcomes of FFRCT, JACC Cardiovasc. Imaging 13 (1) (2020 Jan) 97–105.
[5] A.R. Ihdayhid, B.L. Norgaard, S. Gaur, J. Leipsic, N. Nerlekar, K. Osawa, et al., Prognostic value and risk continuum of noninvasive fractional flow reserve derived from coronary CT angiography, Radiology 292 (2) (2019 Aug) 343–351.
[6] X. Liu, X. Mo, H. Zhang, G. Yang, C. Shi, W.K. Hau, A 2-year investigation of the impact of the computed tomography–derived fractional flow reserve calculated using a deep learning algorithm on routine decision-making for coronary artery disease management, Eur. Radiol. 31 (9) (2021 Sep 25) 7039–7046.
[7] H. Takagi, J.A. Leipsic, N. McNamara, I. Martin, T.A. Fairbairn, T. Akasaka, et al., Trans-lesional fractional flow reserve gradient as derived from coronary CT improves patient management: ADVANCE registry, J. Cardiovasc. Comput. Tomogr. 16 (1) (2022) 19–26.
[8] Y. Takehara, 4D flow when and how? Radiol. Med. [Internet] 125 (9) (2020 Sep 15) 838–850. Available from: https://doi.org/10.1007/s11547-020-01249-0.
[9] A.J. Barker, P. van Ooij, K. Bandi, J. Garcia, M. Albaghdadi, P. McCarthy, et al., Viscous energy loss in the presence of abnormal aortic flow, Magn. Reson. Med. 72 (3) (2014 Sep) 620–628.
[10] N. Oyama-Manabe, T. Aikawa, S. Tsuneta, O. Manabe, Clinical Applications of 4D Flow MR Imaging in Aortic Valvular and Congenital Heart Disease, Magn. Reson. Med. Sci. 21 (2) (2022) (rev.2021-0030).
[11] M.S.M. Elbaz, M.B. Scott, A.J. Barker, P. McCarthy, C. Malaisrie, J.D. Collins, et al., Four-dimensional virtual catheter: noninvasive assessment of intra-aortic hemodynamics in bicuspid aortic valve disease, Radiology 293 (3) (2019 Dec) 541–550.
[12] D. McLennan, M. Schäfer, A.J. Barker, M.B. Mitchell, R.J. Ing, L.P. Browne, et al., Abnormal flow conduction through pulmonary arteries is associated with right ventricular volume and function in patients with repaired tetralogy of Fallot: does flow quality affect afterload? Eur. Radiol. 33 (1) (2022 Jul 19) 302–311.
[13] J.J. Kim, B.H. Hwang, I.J. Choi, E.H. Choo, S. Lim, J.K. Kim, et al., Impact of diabetes duration on the extent and severity of coronary atheroma burden and long-term clinical outcome in asymptomatic type 2 diabetic patients: evaluation by coronary CT angiography, Eur. Heart J. Cardiovasc. Imaging 16 (10) (2015 Oct) 1065–1073.
[14] N. Tomizawa, T. Nojo, S. Inoh, S. Nakamura, Difference of coronary artery disease severity, extent and plaque characteristics between patients with hypertension, diabetes mellitus or dyslipidemia, Int. J. Cardiovasc. Imaging 31 (1) (2015) 205–212.
[15] N. Tomizawa, S. Inoh, T. Nojo, S. Nakamura, The association of hemoglobin A1c and high risk plaque and plaque extent assessed by coronary computed tomography angiography, Int. J. Cardiovasc. Imaging [Internet] 32 (3) (2016 Mar 13) 493–500. Available from: https://doi.org/10.1007/s10554-015-0788-6.
[16] T. Kuzuya, S. Nakagawa, J. Satoh, Y. Kanazawa, Y. Iwamoto, M. Kobayashi, et al., Report of the committee on the classification and diagnostic criteria of diabetes mellitus, Diabetes Res. Clin. Pract. 55 (1) (2002 Jan) 65–85.
[17] Japan Atherosclerosis Society, Japan Atherosclerosis Society (JAS) guidelines for prevention of atherosclerotic cardiovascular diseases, J. Atheroscler. Thromb. (2007 Apr) 5–57.
[18] N. Tomizawa, Y. Hayakawa, S. Inoh, T. Nojo, S. Nakamura, Clinical utility of landiolol for use in coronary CT angiography, in: Research Reports in Clinical Cardiology [Internet] 145, 2015 Nov. Available from: https://www.dovepress.com/clinical-utility-of-landiolol-for-use-in-coronary-ct-angiography-peer-reviewed-article-RRCC.
[19] N. Tomizawa, K. Yamamoto, S. Inoh, T. Nojo, S. Nakamura, Simplified Bernoulli formula to predict flow limiting stenosis at coronary computed tomography angiography, Clin. Imaging 51 (2018 Sep) 104–110.
[20] N. Tomizawa, Y. Nozaki, S. Fujimoto, D. Takahashi, A. Kudo, Y. Kamo, et al., A phantom and in vivo simulation of coronary flow to calculate fractional flow reserve using a mesh-free model, Int. J. Cardiovasc. Imaging [Internet] (2021 Nov 2), https://doi.org/10.1007/s10554-021-02456-0. Available from:.
[21] N. Tomizawa, S. Fujimoto, T. Mita, D. Takahashi, Y. Nozaki, R. Fan, et al., Coronary artery vorticity to predict functional plaque progression in participants with type 2 diabetes mellitus, Radiol. Cardiothorac. Imaging 5 (4) (2023 Aug 1).
[22] A. Imanparast, N. Fatouraee, F. Sharif, The impact of valve simplifications on left ventricular hemodynamics in a three dimensional simulation based on in vivo MRI data, J. Biomech. 49 (9) (2016 Jun) 1482–1489.
[23] K.B. Won, B.K. Lee, F.Y. Lin, M. Hadamitzky, Y.J. Kim, J.M. Sung, et al., Glycemic control is independently associated with rapid progression of coronary atherosclerosis in the absence of a baseline coronary plaque burden: a retrospective case–control study from the PARADIGM registry, Cardiovasc. Diabetol. 21 (1) (2022 Nov 12) 239.
[24] M. Hadamitzky, S. Taubert, S. Deseive, R.A. Byrne, S. Martinoff, A. Schomig, et al., Prognostic value of coronary computed tomography angiography during 5 years of follow-up in patients with suspected coronary artery disease, Eur. Heart J. 34 (42) (2013 Nov 2) 3277–3285.
[25] B.L. Nørgaard, C.J. Terkelsen, O.N. Mathiassen, E.L. Grove, H.E. Bøtker, E. Parner, et al., Coronary CT angiographic and flow reserve-guided management of patients with stable ischemic heart disease, J. Am. Coll. Cardiol. 72 (18) (2018 Oct) 2123–2134.
[26] J.M. Lee, G. Choi, B.K. Koo, D. Hwang, J. Park, J. Zhang, et al., Identification of high-risk plaques destined to cause acute coronary syndrome using coronary computed tomographic angiography and computational fluid dynamics, JACC Cardiovasc. Imaging 12 (6) (2019 Jun) 1032–1043.
[27] N. Tomizawa, Y. Nozaki, S. Fujimoto, D. Takahashi, A. Kudo, Y. Kamo, et al., Coronary flow disturbance assessed by vorticity as a cause of functionally significant stenosis, Eur. Radiol. [Internet] 32 (10) (2022 Jul 2) 6859–6867. Available from: https://doi.org/10.1007/s00330-022-08974-2.
[28] Y. Shiina, K. Inai, S. Miyazaki, M. Nagao, Aortic Vorticity, Helicity, and Aortopathy in Adult Patients with Tetralogy of Fallot: Pilot Study Using Four-Dimensional Flow Magnetic Resonance Images. Pediatr Cardiol [Internet], 2020 Sep 25, https://doi.org/10.1007/s00246-020-02466-0. Available from:.
[29] H. Samady, D.S. Molony, A.U. Coskun, A.S. Varshney, B. de Bruyne, P.H. Stone, Risk stratification of coronary plaques using physiologic characteristics by CCTA: focus on shear stress, J. Cardiovasc. Comput. Tomogr. [Internet] 14 (5) (2020 Sep) 386–393. Available from: https://linkinghub.elsevier.com/retrieve/pii/S1934592519301212.
[30] A. Kumar, E.W. Thompson, A. Lefieux, D.S. Molony, E.L. Davis, N. Chand, et al., High coronary shear stress in patients with coronary artery disease predicts myocardial infarction, J. Am. Coll. Cardiol. [Internet] 72 (16) (2018 Oct) 1926–1935. Available from: https://linkinghub.elsevier.com/retrieve/pii/S0735109718369432.
[31] J. Lantz, V. Gupta, L. Henriksson, M. Karlsson, A. Persson, C.J. Carlhäll, et al., Intracardiac flow at 4D CT: comparison with 4D flow MRI, Radiology 289 (1) (2018 Oct) 51–58.